

AN EXPERIMENTAL EVALUATION OF AUTOMATIC CLASSIFICATION OF SEQUENCES REPRESENTING SHORT CIRCUITS IN TRANSMISSION LINES

JEFFERSON MORAIS*, YOMARA PIRES[†], CLAUDOMIR CARDOSO[‡], ALDEBARO KLAUTAU[§]

**Federal University of Pará, Signal Processing Laboratory (LaPS),
DEEC - CT - UFPA - Belém, Brazil, CP 8619 - 66075-110.*

Emails: jmorais@ufpa.br, yomara@ufpa.br, claudomir@ufpa.br, aldebaro@ufpa.br

Abstract— This work concerns automatic classification of short circuits in transmission lines. These faults are responsible for the majority of the disturbances and cascading blackouts. Each short circuit is represented by a sequence (time-series) and both online (for each short segment) and offline (taking in account the whole sequence) classification are investigated. Results with different preprocessing (e.g., wavelets) and learning algorithms are presented, which indicate that decision trees and neural networks outperform the other methods. Another contribution of this work is to promote the adoption of a public and comprehensive labeled dataset with short circuit sequences, which allows to properly compare the algorithms and reproduce the results.

Keywords— Fault classification, sequence classification, machine learning.

1 Introduction

The electric power industry has currently a reasonably sophisticated logistics to acquire and store time series (waveforms) corresponding to power quality (PQ) [1, 2] events. A typical example is the oscillography equipments [3] that store waveforms along with additional information such as date and time, in cases where the amplitude differs from its nominal value.

More specifically in the fault analysis field, the companies are integrating their legacy supervisory control and data acquisition (SCADA) systems, which report time to the second and do not provide waveforms, with the so-called intelligent electronics devices (IEDs) such as digital fault recorder (DFRs) and digital relays, which can support sampling frequencies of tens of kHz and implement sophisticated algorithms [3]. In both fields, classification and other data mining tasks can be performed at the level of the IED (online) or at a supervisory center (postfault), which collects data from several sources.

This work investigates a particular and important class of causes of PQ events: faults in transmission lines. Studies showed that these faults were responsible for 70% of the disturbances and cascading blackouts [4, 5].

Due to the lack of freely available and standardized benchmarks, most previous publications in this area used proprietary datasets, making difficult to compare algorithms and reproduce results. Another contribution of this work is to promote UFPAFaults2, a public and comprehensive labeled dataset with short circuit sequences, which allows to properly compare the algorithms. The faults of this datasets were simulated with the Alternative Transients Program (ATP) [6]. ATP models have a long history of good reputation with respect to mimicking the actual system behavior when well tuned. Data mining techniques (preprocessing and machine learning algorithms) are

then used to train and test classifiers.

Most of the literature in faults classification (see, e.g., [4]) adopts a raw or wavelet front end and neural networks as the learning algorithm. This work compares the neural networks with decision trees and other classifiers, assuming raw and wavelet front ends.

This paper is organized as follows. Section 2 presents definitions and the notation. Section 3 describes the simulation setup, including the dataset of faults and the adopted algorithms (preprocessing and learning). The simulation results are discussed in Section 4, while Section 5 presents the conclusions.

2 Classification of Time Series Representing Faults

In this work, the time series represent faults, which are basically short-circuits in transmission lines. This section defines a notation that may look abusive. However, there are many ways of representing and classifying time series, and a precise notation is necessary to avoid obscure points.

Most transmission systems use three *phases*: A, B and C. Hence, a short-circuit between phases A and B will be identified as “AB”. Considering the possibility of a short-circuit to “ground” (G), the task is to classify a time series into one among eleven possibilities: AG, BG, CG, AB, AC, BC, ABC, ABG, ACG, BCG, ABCG. Algorithms to solve this classification problem are used by DFRs, distance relays and other equipments (see, e.g., [3]).

The signal capturing equipments are sometimes located at both endpoints of the transmission line. Most of them are capable of digitizing voltage and current waveforms. It is assumed that each equipment has a trigger circuit that detects an anomaly and stores only the interval of interest - the fault and a pre-determined number of

samples before and after the fault. The trigger itself corresponds to a binary classification problem: “fault” or “no-fault” [7], but this interesting problem is out of the scope of the present work.

Each fault is a variable-duration multivariate time-series. The n -th fault \mathbf{X}_n in a dataset (oscillography records, for example) is represented by a $Q \times T_n$ matrix. A column \mathbf{x}_t of \mathbf{X}_n , $t = 1, \dots, T_n$, is a multidimensional *sample* represented by a vector of Q elements. For example, this work adopts $Q = 6$ (voltage and current of phases A, B and C) in the experiments. In some situations [4], it is possible to obtain *synchronized samples* from both endpoints of a given line. In these cases the sample is an augmented vector with twice the dimension of the single endpoint scenario.

A sample composed by the measured currents and voltages is called *raw*. Alternatively, parametric representations such as wavelets [8] can be used.

Independent of the adopted parametric representation, a single sample typically does not carry enough information to allow performing reasonable decisions. Hence, the samples are often concatenated or averaged to create a *frame* \mathbf{F} . Frames have dimension $Q \times L$, where L is the *frame length* and their concatenation $\hat{\mathbf{Z}} = [\mathbf{F}_1 \dots \mathbf{F}_N]$ is a matrix of dimension $Q \times LN$, where N is the number of frames of the fault.

The frames can overlap in time such that the *frame shift* S , i.e. the number of samples between two consecutive frames, is less than the frame length. Hence, the number of frames for a fault \mathbf{X}_n is $N_n = 1 + \lfloor (T_n - L)/S \rfloor$, where $\lfloor \cdot \rfloor$ is the flooring operation. It should be noticed that, if $S = L$ (no overlap between frames) and a frame is a *concatenation of samples* $\mathbf{F} = [\mathbf{x}_{t-0.5(L-1)}, \dots, \mathbf{x}_{t-1}, \mathbf{x}_t, \mathbf{x}_{t+1}, \dots, \mathbf{x}_{t+0.5(L-1)}]$, the matrices $\mathbf{X} = \hat{\mathbf{Z}}$ coincide.

The frames can be conveniently organized as vectors of dimension $K = QL$, and $\hat{\mathbf{Z}}$ resized to create $\mathbf{Z} = [\mathbf{z}_1 \dots \mathbf{z}_N]$ of dimension $K \times N$. It is assumed hereafter that the processing is performed on \mathbf{Z} (not \mathbf{X}).

For example, for $Q = 6$ raw currents and voltages, frames \mathbf{F} of dimension 6×5 could be obtained by concatenation of samples, e.g., taking for each central sample, its two neighbors at left and the two at its right. In this case, assuming $S = L = 5$ and a fault with $T = 10$ samples, $\mathbf{X} = \hat{\mathbf{Z}}$ would have dimension 6×10 , while \mathbf{Z} would be a 30×2 matrix. In practical systems, one can adopt $Q = 6$ and $K = 198$ [4].

Fault classification systems can be divided into two types. The first one aims at performing a decision (classification) for each frame \mathbf{F} . This is typically the goal in on-line scenarios, at the level of, e.g. a protection relay [4]. On-line fault classification must be performed on a very short time span. It is often based on a frame corresponding

to half or one cycle of a sinusoidal signal of 60 or 50 Hz. Assuming, 60 Hz and a sampling frequency of $f_s = 2$ kHz, one cycle corresponds to $L = 2000/60 \approx 33$ samples. Alternatively, the decision can be made at a supervisory center in a post-fault stage. The latter case deals with matrices \mathbf{Z} of variable dimension $K \times N_n$, while the former with vectors \mathbf{z} of a fixed dimension K . The on-line and post-fault systems try to solve problems that can be cast as *conventional classification* [9] and *sequence classification* [10] problems, respectively.

In a conventional classification scenario, one is given a *training set* $\{(\mathbf{z}_1, y_1), \dots, (\mathbf{z}_M, y_M)\}$ containing M *examples*. Each example (\mathbf{z}, y) consists of a vector $\mathbf{z} \in \mathbb{R}^K$ called *instance* and a *label* $y \in \{1, \dots, Y\}$. A *conventional classifier* is a mapping $\mathcal{F} : \mathbb{R}^K \rightarrow \{1, \dots, Y\}$. Some classifiers are able to provide *confidence-valued scores* $f_i(\mathbf{z})$ for each class $i = 1, \dots, Y$, such as a probability distribution over y . For convenience, it is assumed that all classifiers return a vector \mathbf{y} with Y elements. If the classifier does not naturally return confidence-valued scores, the vector \mathbf{y} is created with a unitary score for the correct class $f_y(\mathbf{z}) = 1$ while the others are zero $f_i(\mathbf{z}) = 0, i \neq y$. The final decision is based on the max-wins rule $\mathcal{F}(\mathbf{z}) = \arg \max_i f_i(\mathbf{z})$.

Contrasting to the on-line case, the post-fault classifier is a mapping $\mathcal{G} : \mathbb{R}^{K \times N_n} \rightarrow \{1, \dots, Y\}$ and the training set $\{(\mathbf{Z}_1, y_1), \dots, (\mathbf{Z}_M, y_M)\}$ contains M sequences and their labels.

There are techniques for implementing \mathcal{G} that deal directly with sequences, such as hidden Markov models (HMM) [11] and dynamic time-warping (DTW) [12]. Another alternative is the *frame-based sequence classification* (FBSC) architecture, in which the fault module repeatedly invokes a conventional classifier F (e.g., neural network or decision tree) to obtain the scores $\mathbf{y} = (f_1(\mathbf{z}), \dots, f_Y(\mathbf{z}))$ for each class. To come up with the final decision, the fault module can then take in account the scores of all frames. For example, the module can calculate an accumulated score $g_i(\mathbf{Z})$ for each class and then use the max-wins rule

$$G(\mathbf{Z}) = \arg \max_i g_i(\mathbf{Z}),$$

where possible alternatives are:

$$g_i(\mathbf{Z}) = \sum_{n=1}^N f_i(\mathbf{z}_n) \quad (1)$$

or

$$g_i(\mathbf{Z}) = \sum_{n=1}^N \log(f_i(\mathbf{z}_n)). \quad (2)$$

In FBSC, the accuracy of $G(\mathbf{Z})$ is clearly dependent on the accuracy of the classifier $\mathcal{F}(\mathbf{z})$.

The performance of the fault classifiers can be evaluated according to their misclassification

rates E_s and E_f , for the sequence (post-fault) and frame-by-frame (on-line) modules, respectively.

One can see that there are many degrees of freedom when designing an algorithm for fault classification. The next section presents the framework adopted.

3 Simulation Setup

The simulations used the UFPAFaults2 dataset, which can be downloaded from www.laps.ufpa.br/freedatasets/UfpaFaults/. This dataset is composed by 1.000 simulated faults, which were split into two disjoint sets with 500 examples each, to be used for training and testing. An explanation about how the faults are generated with the software AmazonTP is given in [13].

3.1 Preprocessing and front end

It is beneficial to normalize the raw data such that the waveforms have amplitudes approximately in the range $[-1, 1]$ (per unit or *pu*). This work used two types of normalization, which are called here *prefault* and *allfault*. In the *prefault* normalization, a fixed-duration interval of the signal preceding the disturbance is used to find the maximum absolute value X_{\max} . Then, this maximum value is used as base for the conversion of each phase to *pu*. The *allfault* normalization takes in account all duration of the waveforms for getting the maximum and minimum amplitudes of each phase, and the converting to *pu*. Both normalizations adopt a distinct normalization factor for each of the Q waveforms. For example, if one waveform has an overshoot of amplitude X_{\max} , the *allfault* can convert X_{\max} to 1 and keep the whole waveform in the $[-1, 1]$ range, while *prefault* may convert X_{\max} to a value much larger than 1, because its normalization factor is based on a pre-fault interval (where the amplitudes are typically close to their nominal values).

After the analog to digital conversion and preprocessing, the *front end* is responsible by all operations to generate the sequence that will be passed to the mining algorithms (e.g., classification and clustering). All front ends in this work assume an input sequence \mathbf{X} with $Q = 6$ raw currents and voltages at $f_s = 40$ kHz.

Wavelet is a popular representation for fault classification [14]. There are many ways of representing a sequence through wavelet coefficients. In this work, two front ends based on wavelets are investigated.

Some works in the literature use only one of the details or calculate the average power of the coefficients [15]. In contrast, the *waveletconcat* front end concatenates all the coefficients and organizes them in a matrix \mathbf{Z} . One has to take in account that the coefficients have different sam-

pling frequencies. For example, assuming a 3-level decomposition of a signal with $f_s = 2$ kHz, there are four signals (sequence of coefficients) for each of the Q waveforms: the approximation \mathbf{a} , and three details \mathbf{d}_1 , \mathbf{d}_2 and \mathbf{d}_3 , which have sampling frequencies, given by 250, 1000, 500, 250, respectively. Therefore, instead of using a single L , the *waveletconcat* front end adopts a value L_{\min} for the signals with lowest f_s (\mathbf{a} and \mathbf{d}_3 in the previous example). The other signals use a multiple of L_{\min} . Invoking the previous example again, $L = 8L_{\min}$ and the frame lengths for \mathbf{d}_1 and \mathbf{d}_2 are $4L_{\min}$ and $2L_{\min}$, respectively.

A similar reasoning is applied to the shift S , which requires the definition of S_{\min} .

The coefficients are then organized in a frame \mathbf{F} of dimension $Q \times L$, where $L = 2^k L_{\min}$ for a decomposition level k . The number of frames is given by

$$N = 1 + \lfloor (T_a - L_{\min}) / S_{\min} \rfloor,$$

where T_a is the number of elements in \mathbf{a} .

Another alternative for organizing the wavelet coefficients is by taking the windowed normalized total energy (average power) of each coefficient. This front end is called *waveletenergy* and, similarly to the *waveletconcat*, it has to deal with signals of different sampling frequencies. Their main distinction is that, instead of concatenating all coefficients, *waveletenergy* represents \mathbf{X} by its energy (or power) in frequency bands specified by the wavelet decomposition. Hence, *waveletenergy* loses information but can achieve a significant reduction in computational cost of the classification algorithms by decreasing the number of parameters.

3.2 Learning Algorithms

The simulations in this paper relied on Weka [9], which has many learning algorithms. Specifically, the work used decision trees (J4.8, which are a Java version of C4.5 [9]), multilayer artificial neural network (ANN) trained with backpropagation, naive Bayes and K-nearest neighbor (KNN) [9]. For KNN, instead of using the whole dataset in the test stage, the K-means clustering algorithm was adopted for finding a specified number of centroids to represent the training set [9]. This can substantially reduce the computational cost of KNN. A discriminative Gaussian Mixtures (GMM) classifier [16] was also adopted, which estimates a mixture of Gaussians for each class.

These classifiers were used for on-line fault classification experiments, where the decisions are made on a frame-by-frame basis. For post-fault classification, among the several options (HMM, DTW, etc.), this work adopts FBSC architectures by modifying the Weka code [9] to invoke the previous classifiers.

Table 1: Approximate computational cost for some classifiers, where *sigm* is a sigmoid function and *mac* is a multiply and add operation, executed in one cycle in modern DSP chips.

Classifier	Cost
J4.8	$\log_2 p_n$ if-else
ANN	$(Y + p_h)$ sigm, $(K + Y)p_h$ mac
KNN	$p_m K$ mac
GMM	$Y p_g K$ mac
Naive Bayes	$Y K$ mac

It is interesting to compare the computational cost of the classifiers during the test stage. The training stage can be done offline and is typically less important. The cost depends on the complexity of each classifier and can be roughly estimated as follows. A binary decision tree as J4.8 with p_n internal nodes requires $\log_2(p_n)$ comparisons to reach a leaf. Assuming ANNs with one hidden layer of p_h nodes, each node computes an internal product between vectors of dimension $K + 1$ (input dimension plus bias) and calls a sigmoid function. Similar work is done by each of the Y nodes of the output layer, but with vectors of dimension p_h . A KNN classifier using p_m stored vectors (training instances or centroids calculated by clustering) and the Euclidean distance, requires computing p_m internal products or, alternatively, p_m squared norms of vectors of dimension K . Assuming each of the Y classes being modeled by a mixture with p_g Gaussians, the GMM classifier requires $Y p_g$ Euclidean distances for calculating log-likelihoods. When the Naive Bayes classifier uses a one-dimensional Gaussian for each element of the input \mathbf{z} (as in this work), its cost is equivalent to a GMM with one Gaussian per class. This rough estimate of the total cost at the test stage of these classifiers is summarized in Table 1.

To provide a single cost estimate, the table suggested in [17] was used to weight the different operations (arithmetic, logical, etc.). These weight obviously depend very much on the computing platform but they are helpful to provide a first approximation.

3.3 Parameter selection

Often, the best performance on a particular dataset can only be achieved by tedious parameter tuning. This is a computational intensive approach, but avoids tuning the parameters by repeatedly evaluating the classifier using the test set. A popular strategy is to perform this parameter (or model) selection using cross-validation.

It should be noted that, conventionally, the examples are assumed to be independently and identically distributed (iid) “samples” from an unknown but fixed distribution $P(\mathbf{z}, y)$. However,

Table 2: Front end parameters ($Q = 6$ and the wavelet is db4 with 3-levels).

Front end	Parameters
raw	$L = 9, S = 9, K = 54$
waveletconcat	$L_{\min} = 4, S_{\min} = 2, K = 192$
waveletenergy	$L_{\min} = 1, S_{\min} = 1, K = 24$

this assumption is invalid when training and test datasets of fault classification experiments can have vectors \mathbf{z} extracted from the same sequence. This fact is important in practice because when performing model selection based on, e.g. cross-validation, the procedure can lead to overfitting because vectors that were extracted from the same waveform have relatively high similarity among them.

Because of that, automatic model selection used a validation file disjunct with respect to the train and test files. Combinations of possible parameters were specified as a *grid* and searched exhaustively.

4 Experimental Results

In the preprocessing stage, the 40 kHz waveforms were decimated by 20 to create sequences with $f_s = 2$ kHz.

Results for the three different front ends in Table 2 are discussed. The first front end, which is called *raw*, adopts $L = 9$ raw samples (central, four at the left and four at the right), such that $K = 54$. There is no overlap ($S = L$). The two wavelet front ends used a Daubechies 4 (db4) [8] with a 3-level decomposition. Hence, for each of the $Q = 6$ waveforms, the wavelet decomposition generated four signals. The waveletconcat adopted $L_{\min} = 4$ and $S_{\min} = 2$, while waveletenergy used $L_{\min} = S_{\min} = 1$. For example, Assuming a 6×5000 matrix \mathbf{X} (already at $f_s = 2$ kHz), waveletconcat generates a sequence \mathbf{Z} with $K = 192$ and $N = 311$ frames. Table 3 indicates the parameters of the classifiers obtained by the automatic model selection procedure.

Figure 1 shows a comparison between the two normalization methods adopted in this work. For both, the best results were obtained by the ANN and J4.8 classifiers. The large difference for the Naive Bayes classifiers requires further analysis.

Figure 2 shows the results for the two wavelet front ends (the results for the raw are repeated for convenience). These two did not outperform the best result obtained with the front end *raw*. One should notice, however, that there are many degrees of freedom when designing a front end based on the wavelet transform, and these should be seen as baseline results.

Figure 3 indicates the estimated computational cost of some classifiers. Model selection

Table 3: Parameters of the classifiers designed by the automatic model selection procedure for the default normalization.

Front end	Classifier	Parameter
raw ($K = 54$)	ANN	$p_h = 32$
	J4.8	$p_n = 258$
	Naive Bayes	-
	KNN	$p_m = 1111$
	GMM	$p_g = 8$
wavelet-concat ($K = 192$)	ANN	$p_h = 16$
	J4.8	$p_n = 413$
	Naive Bayes	-
	KNN	$p_m = 1111$
	GMM	$p_g = 1$
wavelet-energy ($K = 24$)	ANN	$p_h = 36$
	J4.8	$p_n = 287$
	Naive Bayes	-
	KNN	$p_m = 1100$
	GMM	$p_g = 4$

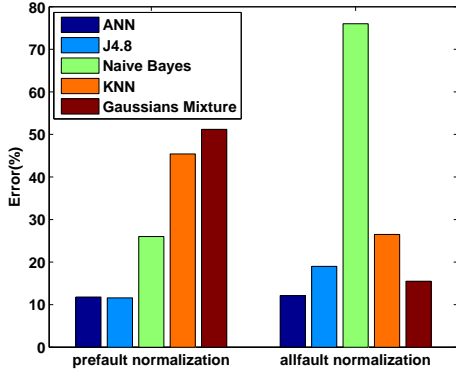


Figure 1: Error rate E_f using the raw front end and different normalization strategies.

chooses different classifiers when the normalization strategy changes. An exception is the Naive Bayes classifier, which does not have such parameters and presents the same cost.

Some FBSC post-fault classifiers G were designed using Eq. (1) and the max-wins rule. Figure 4 shows $E_f - E_s$, the absolute reduction in error rate when comparing sequence classification and the corresponding conventional classification. For example, the GMM presents $E_f = 51.3\%$ and $E_s = 31.6\%$, which leads to a difference of 19.7%.

Figure 5 shows a comparison of the robustness of the J4.8 and ANN classifiers to the addition of white Gaussian noise (AWGN) to the waveforms. Both classifiers were trained with waveforms not contaminated by noise and tested under a condition of a signal to noise ratio of 30 dB, i.e. a forced mismatch condition between train and test. It can be seen that in this case, J4.8 was slightly less robust to noise than the ANN.

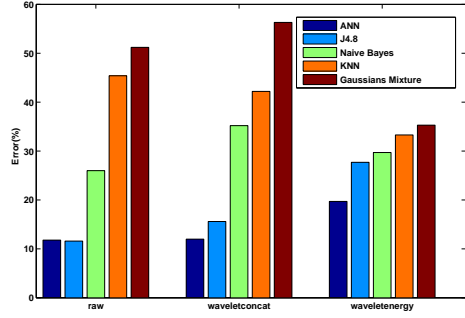


Figure 2: Error rate E_f of front ends **waveletenergy**, **waveletconcat** and **raw** (the first set of results is the same as in Fig. 1).

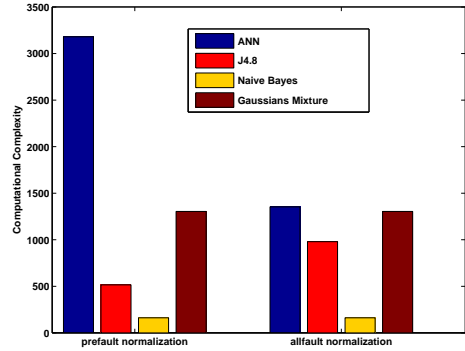


Figure 3: Computational cost of the test stage estimated using the table suggested in [17] for the best classifiers found by the model selection procedures, for pre-fault and all-fault normalizations. The cost of the KNN classifiers were around 180,000.

5 Conclusions

This paper presented a thorough description of the issues related to the design of fault classification modules for power electric systems. The solutions to this problem involve digital signal processing and machine learning algorithms. Consequently, there are many degrees of freedom when designing a classifier. For example, the wavelets front ends would probably benefit from finer tuning.

The experimental results indicated that neural networks and decision trees outperformed the other classifiers. Decision trees seem particularly interesting when one is trying to minimize the computational cost, such as in the development of embedded devices. Neural networks achieved a better accuracy and improved robustness.

The post-fault classification deserves more investigation. The FBSC architecture is just one among many options. It is interesting that a GMM classifier, which outputs log-likelihoods, had a large discrepancy between E_s and E_f , while the difference was much smaller for ANN. This is another topic that deserves further investigation.

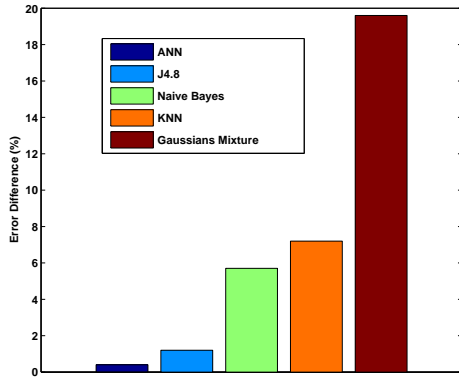


Figure 4: Difference $E_f - E_s$ between the error rates for frame-by-frame and sequence classification using pre-fault normalization and the raw front end.

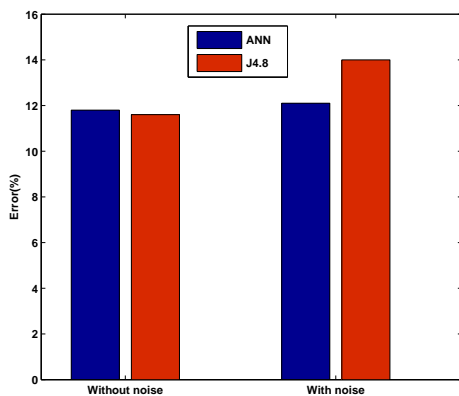


Figure 5: Difference between datasets with noise and without noise (the first set of results is the same as in Fig. 1).

Acknowledgements

Thanks to Eletronorte and Prof. Marcus Nunes (GSEI/UFPA) for sharing the ATP models.

References

- [1] S. Santoso and J.D. Power Lamoree. Power quality data analysis: From raw data to knowledge using knowledge discovery approach. In *Engineering Society Summer Meeting, IEEE*, pages 172–177, 2000.
- [2] Slavko Vasilic. *Fuzzy Neural Network Pattern Recognition Algorithm for Classification of the Events in Power System Networks*. PhD thesis, Texas A&M University, 2004.
- [3] X. Luo and M. Kezunovic. Fault analysis based on integration of digital relay and dfr. *Power Engineering Society General Meeting*, 1:746 – 751, 2005.
- [4] N. Zhang and M. Kezunovic. A real time fault analysis tool for monitoring operation

- of transmission line protective relay. *Electric Power Systems Research*, 77:361–70, 2007.
- [5] Math H.J. Bollen. *Understanding power quality problems: Voltage sags and interruptions*. IEEE Press Series on Power Engineering, 2000.
- [6] EMTP. *Alternative Transients Program (ATP) Rule Book*. Canadian/American EMTP User’s Group, 1995.
- [7] A. McEachern. A floating-window algorithm for detecting certain power line faults that disrupt sensitive electronic loads. *Instrumentation and Measurement, IEEE Trans.*, 39:112–115, 1990.
- [8] M. Vetterli and J. Kovačević. *Wavelets and Subband Coding*. Prentice Hall, 1995.
- [9] I. Witten and E. Frank. *Data Mining: Practical Machine Learning Tools and Techniques with Java Implementations*. Morgan Kaufmann, 2nd Edition, 2005.
- [10] Ming Li and R Sleep. A robust approach to sequence classification. In *International Conference on Tools with Artificial Intelligence*, page 5, 2005.
- [11] L. Rabiner. A tutorial on hidden Markov models and selected applications in speech recognition. *Proceedings of the IEEE*, 77(2):257–86, Feb. 1989.
- [12] H. Sakoe and S. Chiba. Dynamic programming algorithm optimization for spoken word recognition. *IEEE Trans. on ASSP*, 26(1):43–49, 1978.
- [13] Yomara Pires et al. A framework for evaluating data mining techniques applied to power quality. In *Brazilian Conference on Neural Networks (CBRN)*, 2005.
- [14] Y. Wu and M. Kezunovic. Automatic simulation of IED measurements for substation data integration studies. *IEEE PES 2005 General Meeting*, 3:2556 – 2561, 2005.
- [15] C.Aguilera, E.Orduna, and G.Rattá. Fault detection, classification and faulted phase selection approach based on high-frequency voltage signals applied to a series-compensated line. *IEEE Proc.- Gener. Transm. Distrib.*, 153:469–475, 2006.
- [16] A. Klautau et al. Discriminative Gaussian mixture models: A comparison with kernel classifiers. In *ICML*, pages 353–360, 2003.
- [17] J. R. Boisson de Marca. An LSF quantizer for the north-american half-rate speech coder. *IEEE Transactions on Vehicular Technology*, 43:413–419, 1994.